Multi-omics-based analysis of the regulatory mechanism of gypenosides on bile acids in hypercholesterolemic mice

CHENGCHENG FENG[1], YANPING YANG[1], ANJING LU[2], DAOPENG TAN[1,2], YANLIU LU[1,2], LIN QIN[1,2] and YUQI HE[1,2]

[1]Joint International Research Laboratory of Ethnomedicine of Ministry of Education; [2]Guizhou Engineering Research Center of Industrial Key-Technology for Dendrobium Nobile, Zunyi Medical University, Zunyi, Guizhou 563000, P.R. China

Received December 1, 2022; Accepted June 22, 2023

DOI: 10.3892/etm.2023.12136

Abstract. *Gynostemma pentaphyllum* is a traditional medicine used by ethnic minorities in southwest China and gypenosides are currently recognized as essential components of the pharmacological substances of *Gynostemma pentaphyllum*, which are effective in regulating metabolic syndrome, especially in improving hepatic metabolic disorders. The present study randomly divided C57BL/6J male mice into the normal diet control group (ND), high-fat diet modeling group (HFD) and gypenosides group (GP). Liquid chromatography-mass spectrometry (UPLC-MS) was applied to quantify bile acids in the liver, bile and serum of mice in ND, HFD and GP groups. Liver proteins were extracted for trypsin hydrolysis and analyzed quantitatively using UPLC-MS + MS/MS (timsTOF Pro 2). Total mouse liver RNA was extracted from ND, HFD and GP groups respectively, cDNA sequencing libraries constructed and sequenced using BGISEQ-500 sequencing platform. The expression of key genes *Fxr*, *Shp*, *Cyp7a1*, *Cyp8b1*, and *Abab11* was detected by RT-qPCR. The results showed that gypenosides accelerated free bile acid synthesis by promoting the expression of bile acid synthase CYP7A1 and CYP8B1 genes and proteins and accelerating the secretion of conjugated bile acids from the liver to the bile ducts. GP inhibited the bile acid transporters solute carrier organic anion transporter family member (SLCO) 1A1 and SLCO1A4, reducing the reabsorption of free bile acids and accelerating the excretion of free bile acids from the blood to the kidneys. It also promoted the metabolic enzyme CYP3A11, which accelerated the metabolism and clearance of bile acids, thus maintaining the balance of the bile acid internal environment.

Correspondence to: Professor Yuqi He, Joint International Research Laboratory of Ethnomedicine of Ministry of Education, Zunyi Medical University, 6 Xuefu West Road, Zunyi, Guizhou 563000, P.R. China
E-mail: yqhe.pharm@foxmail.com

Key words: gypenosides, hypercholesterolemia, bile acid, multi-omics analysis

Introduction

Hypercholesterolemia is a metabolic disease with dyslipidemia and can be divided into two categories: One is based on genetics including familial and polygenic hypercholesterolemia; the second is based on elevated lipoproteins (1), which are mainly manifested by abnormally elevated serum or plasma levels of total cholesterol (TC) and low-density lipoprotein cholesterol (LDL-C) (2). Obesity and diet are important factors in causing elevated lipoproteins, especially foods that are high in saturated fatty acids and high in saturated cholesterol (3). Statins are commonly used drugs for the treatment of hypercholesterolemia (4) but are accompanied by serious adverse reactions (5), such as liver dysfunction, rhabdomyolysis and increased susceptibility to diabetes (6). Therefore, it is urgent to find other lipid-regulating drugs to reduce the occurrence of adverse drug reactions.

The Chinese Herbal Medicine *Gynostemma pentaphyllum* (Thunb.) Makino is the dried whole herb of *Gynostemma pentaphyllum*, family Cucurbitaceae. Gypenosides (GP), the main active ingredient of *G. pentaphyllum*, can significantly reduce blood lipid levels (7). Megalli *et al* (8) found that following 12 days of oral administration the gypenosides extract (250 mg/kg) reduced TC and TG levels in rats and no adverse effects were found with long-term oral administration of large doses (9,10). Gypenosides possess a core structure of Dammaran-type triterpenes, similar to the core structure of endogenous bile acids (7). Bile acids are the main product of cholesterol metabolism. Excess cholesterol in the liver is essential for hepatic protection by converting it into bile acids that enter the bile ducts, maintain cholesterol homeostasis and prevent cholesterol accumulation in the liver (11). Cholesterol metabolism is closely related to the processes of bile acid synthesis, metabolism and transport, which are influenced by proteins and genes related to the bile acid pathway.

Bile acids are found mainly in the liver and are mediated by CYP7A1, CYP8B1 and various enzymes for hepatic cholesterol to cholic acid (CA) and chenodeoxycholic acid (CDCA) (12), coupled with taurine or glycine to form bound bile acids taurine/glycine-conjugated cholic acid (T/G-CA), taurine/glycine-conjugated chenodeoxycholic acid (T/G-CDCA) (13-15). The bile acid efflux transporter bile

salt export pump (ABCB11) is responsible for mediating the transport of free and conjugated bile acids from hepatocytes to the gallbladder. solute carrier organic anion transporter family member (SLCO) 1A1 is expressed in the basement membrane of hepatocytes in the portal vein, where it is thought to be a bidirectional transporter protein that transports free saprophytic acid and organic anions into the blood (16,17). SLCO1A1 is expressed on the basal hepatocytes of the hepatic sinusoids and is responsible for the translocation and reabsorption of free bile acids from the blood into the liver (18), where they are eventually excreted through the body's circulation. In addition, the nuclear receptor farnesoid X receptor (FXR) acts as a bile acid receptor with a role in regulating glucose metabolism, lipid metabolism and energy metabolism (19). Bile acids maintain cholesterol-bile acids homeostasis by activating hepatic FXR to induce feedback inhibition of CYP7A1 expression by small heterodimer partner (SHP, NR0B2), thereby inhibiting cholesterol metabolism and bile acids synthesis (20,21). NR4A1 is also a key transcription factor for glucose lipid homeostasis and its overexpression attenuates hepatic triglyceride production and regulates a variety of key genes involved in lipid metabolism (22), accelerating the initial phase of lipogenesis by regulating mitosis (23). Hypercholesterolemia upregulates NR4A1expression (24) and NR4A1 may be the upstream molecule of the SHP upstream molecule, which indirectly regulates lipid metabolic processes by regulating transcription factors (25,26).

The present study analyzed the regulatory effects of GP on bile acid pathway and the mechanism of hepatic cholesterol lowering in mice stimulated by HFD through a combination of metabolomics, proteomics and transcriptomics.

Materials and methods

Plant and Materials. Gypenosides (purity >98% assayed by UV) were purchased from Zhongxin Biotechnology (Zhejiang) Co., Ltd. The purity of gypenosides >98% was verified using high-performance liquid chromatography with diode-array detection (HPLC-DAD) as in a previous study (7). The standard reference material of bile acids was bought from MilliporeSigma. TRIzol® was purchased from Thermo Fisher Scientific, Inc. Trypsin-EDTA solution, 0.25% (without phenol red) was purchased from Promega Corporation. Acetonitrile was purchased from Tedia Co., Inc. Trypsin inhibitors were purchased from Calbiochem (Merck KGaA). Iodoacetamide (IAA), 1,4-dithiothreitol (DTT) and urea were purchased from MilliporeSigma. Isopropanol, methanol and trichloromethane were purchased from Chengdu Kelong Chemical Reagent Factory.

Animal experiments. The experimental protocol was approved by the Institutional Animal Care and Use Committee at Zunyi Medical University (approval no. 2-557). Male C57BL/6J mice weighing 23-25 g, 6-8 weeks old, n=90 were kept in a controlled animal room on the SPF level, and were purchased from Beijing Huafukang Biotechnology, approval number: SCXK 2014-0004. Temperature was 21-23˚C and the humidity 50-60%. The animals consumed food and drank water freely and a 12-h light/dark cycle was used. Following an acclimation period of 1 week, the mice were randomly grouped into 3 groups (n=5 per group). One group was fed a normal diet (ND; Research Diets, Inc.; cat. no. D12450B;10% Kcal fat; energy density: 3.82 kcal/g) and the others were fed a high-fat diet (HFD) purchased from Research Diets, Inc.; cat. no. D12492. The processed formula is: Casein 25.84%, L-cystine 0.39%, maltodextrin 16.15%, sucrose 8.90%, cellulose 6.46%, soybean oil 3.23%, lard 31.66%, mineral mixture 1.29%, dicalcium phosphate 1.68%, calcium carbonate 0.71%, potassium citrate 2.13%, vitamin mixture 1.29%, choline Tartaric acid salt 0.26% and dye 0.01%, respectively. According to the previous research of the authors, the hypercholesterolemia model could be built at 16 weeks of HFD (27). One of the HFD groups was treated under intragastric administration with GP (HFD + GP, 250 mg/kg) from weeks 17 to 38, while mice in ND and the other HFD group was treated under intragastric administration with 0.1% of Carboxymethyl-Na solution (medium used to suspend gypenosides in reverses osmosis water, once per/d). After 18, 20, 26, 32 and 38 weeks, mice were injected intraperitoneally using 1.5 g/kg of 20% urethane, then whole blood and liver were taken following anaesthesia. Blood was centrifuged at 4˚C 4,500 g for 10 min after settling at 4˚C for 60 min to isolate serum. All of the other samples were transferred to liquid nitrogen immediately for quick freezing, then moved to a -80˚C refrigerator until testing and analysis.

Lipid assessment and hematoxylin and eosin (HE) staining. The kits for TC and LDL-C assays were purchased from Nanjing Jiancheng Bioengineering Institute and were used according to the manufacturer's instructions. The liver was fixed in 10% neutral formaldehyde at room temperature for 24 h and rinsed under running water. Dehydration was carried out by immersion in ethanol solutions of different concentrations (70, 80, 90, 95 and 100%) for 30 min, respectively. Then, it was soaked in xylene solution and wax in turn (60 min for soft wax, 120 min for soft wax, 120 min for hard wax). It was embedded in a mold and placed on a freezing table and left to cool and solidify rapidly for about 10 min and then removed (modular tissue embed- ding centre; cat. no. EG1150; Leica Microsystems GmbH). Then the blocks were sectioned at 3-5 μm using a Leica RM2245 Biosystems (Leica Microsystems GmbH). Tissue sections were dewaxed and redehydrated before staining with hematoxylin solution for 5 min, rinsed with running water, stained with 0.5% eosin staining solution for 1 min and rinsed with tap water at room temperature. Images were captured at x400 magnification on a light microscope Olympus BX43 (Olympus Corporation).

Metabolomics of GP regulating molecular levels of bile acid in mice. Liver was homogenized and then centrifuged at 4˚C at 12,000 g for 15 min. 250 μl of supernatant was removed and blown dry on a nitrogen blower at room temperature. Rehydrated with 50% methanol in water, centrifuged under the above conditions and 50 μl was taken as the sample to be tested.

A chromatographic column, ACQUITY UPLC BEH C_{18} (1.7 μm, 3.0x150 mm), was used for the separation of bile acids. The flow rate was 0.3 ml/min. The injection volume was 10 μl and the column temperature was 45˚C. Mobile phase A was 20% acetonitrile (containing 5 mmol/l ammonium acetate) and mobile phase B was 80% acetonitrile (containing 5 mmol/l ammonium acetate) with gradient elution. The elution

conditions and the rest of the chromatographic conditions are referred to in a previous study (28) Table I.

The single ion monitoring (SIM) mode was adopted to capture the $[M-H]^-$ ion of expected bile acids (BAs). Peak areas were used for comparison and statistical analysis. The mass spectrometer used an electrospray ionization source (ESI) in negative ion. The ion source parameters were set as gas temp: 326˚C, gas flow: 12 l/min, nebulizer pressure: 55 psi and capillary voltage: 3.5 kV. Detection ion: Taurocholate acid (TCA) $[M-H]^-$ *m/z* 514.1, Tauroursodeoxycholic acid (TUDCA), taurohyodeoxycholic acid (THDCA), Taurochenodeoxycholic acid (TCDCA), tauroursodeoxycholic acid (TDCA) $[M-H]^-$ *m/z* 498.2, taurolithocholic acid (TLCA) $[M-H]^-$ *m/z* 482.1, glycocholic acid (GCA) $[M-H]^-$ *m/z* 464.6, Glycochenodeoxycholic acid (GCDCA), glycodeoxycholic acid (GDCA), glycoursodeoxycholic acid (GUDCA) $[M-H]^-$ *m/z* 448.2, cholic acid (CA) $[M-H]^-$ *m/z* 407.6, ursodesoxycholic acid (UDCA), hyodeoxycholic acid (HDCA), chenodeoxycholic acid (CDCA), deoxycholic acid (DCA) $[M-H]^-$ *m/z* 391.5 and lithocholic acid (LCA) $[M-H]^-$ *m/z* 375.2.

Proteomics of GP regulating bile acid pathway in mouse liver. Samples were removed from -80˚C, added to four times the volume of lysis buffer (1% Triton X-100 and 1% protease inhibitor) and lysed by ultrasonics (25 KHz, ultrasound 5 sec, 10 ec interval, 100 repetitions, samples were placed on ice.) before being centrifuged at 12,000 g for 10 min at 4˚C. Protein concentration was determined using a BCA kit (Beijing Solarbio Science & Technology Co., Ltd.).

Each sample protein was digested by adding an equal amount of standard protein, then adding DTT to a final concentration of 5 mM and reducing at 56˚C for 30 min. Afterwards, IAA was added to a final concentration of 11 mM and incubated for 15 min at room temperature and protected from light. Finally, triethylammonium bicarbonate buffer (TEAB) was added to dilute urea to ensure that the concentration was <2 M. Trypsin was added at a ratio of trypsin: protein=1:50 and digestion performed at 37˚C overnight. The next day, trypsin was added again in the ratio of trypsin: protein=1:100 and the trypsin digestion were continued for 4 h.

The peptides were dissolved with liquid chromatography mobile phase A and then separated using a NanoElute ultra performance liquid phase system. Mobile phase A was 0.1% formic acid solution and mobile phase B was acetonitrile (containing 0.1% formic acid). Liquid phase gradient settings: 0-70 min, 6-24%B; 70-84 min, 24-35%B; 84-87 min, 35-80%B; 87-90 min, 80%B, with the flow rate maintained at 400 nl/min.

The peptides were separated by the Ultra-HPLC system and then injected into the capillary ion source for ionization and then into the TOF Pro mass spectrometer for analysis. The ion source voltage was set to 1.6 kV and the peptide parent ions and their secondary fragments were detected and analyzed using time of flight (TOF). The secondary mass spectrometry scan range was m/z 100-1,700. The data acquisition mode was used in parallel accumulated serial fragmentation (PASEF) mode. A primary mass spectrum acquisition was followed by 10 PASEF mode acquisitions of secondary spectra with parent ion charge numbers in the range of 0-5. The dynamic exclusion time of the tandem mass spectrometry scan was set to 30 sec to avoid repeated scanning of the parent ions.

Table I. Conditions of gradient elution.

Time (min)	20% Acetonitrile + 5 mM Ammonium acetate (%)	80% Acetonitrile + 5 mM Ammonium acetate (%)
0	95	5
5	95	5
14	86	14
14.5	75	25
17.5	75	25
18	50	50
22	50	50
22.5	20	80
24.5	20	80
25	0	100
27	0	100
28	95	5
33	95	5

Secondary mass spectrometry data were retrieved using Maxquant (v1.6.6.0; Max Planck Institute of Biochemistry). The search parameters were set: the database was SwissProt Mouse (17,032 sequences), an inverse library was added to calculate the false positive rate (FDR) due to random matching. A common contamination library was added to the database to eliminate the effect of contaminated proteins in the identification results; the digestion mode was set to Trypsin/P; the number of missed cut sites was set to 2; the first mass error tolerance of the primary parent ion was set to 20 and 20 ppm for search and main search, respectively and the mass error tolerance of the second fragment ion was 0.02 Da. The cysteine alkylation was set to fixed modification, the variable modification to oxidation of methionine and the acetylation of protein *N*-terminal. The FDR for protein identification and PSM identification were set to 1%.

The proteomics KEGG database was searched for its pathway map (PATHWAY: map00120) using Bile acid as a keyword, and proteins associated with bile acid/cholesterol were searched in the NCBI database, resulting in 45 proteins for analysis.

Transcriptomics of GP regulating bile acid pathway in mouse liver. Briefly, liver tissues were lysed using TRIzol® (Thermo Fisher Scientific, Inc.) RNA was extracted with trichloromethane, centrifuged at 12,000 g for 15 min at 4˚C. The supernatant was enriched with isopropyl alcohol and centrifuged at 12,000 g for 15 min at 4˚C. The precipitate was washed with 75% ethanol and centrifuged at 7,500 g for 15 min at 4˚C. The RNA was resolubilized using the appropriate amount of DEPC water and detected by NanoDrop. The concentration and OD 260/280 ratio of total RNA samples were measured by NanoDrop ultra-micro spectrophotometer (NanoDrop Technologies; Thermo Fisher Scientific, Inc.).

After the samples had been extracted, the RNA concentration purity and RNA integrity values were checked with an Agilent 2100 Bioanalyzer (Agilent Technologies, Inc.);

Table II. Primers used for reverse transcription-quantitative PCR.

Gene	Forward primer (5' to 3')	Reverse primer (5' to 3')
Cyp7a1	GAGCCCTGAAGCAATGAAAG	GCTGTCCGGATATTCAAGGA
Cyp8b1	GGACAGCCTATCCTTGGTGA	GACGGAACTTCCTGAACAGC
Fxr	TTCCTCAAGTTCAGCCACAG	TCGCCTGAGTTCATAGATGC
Shp	GGAGTCTTTCTGGAGCCTTG	ATCTGGGTTGAAGAGGATCG
Gapdh	TGTGTCCGTCGTGGATCTGA	CCTGCTTCACCACCTTCTTGA

the screened RNA was reverse transcribed into cDNA for library construction and sequenced and analyzed by using a BGISEQ-500RS RNA-Seq platform (BGI Biotechnology (Wuhan) Co., Ltd.); GRCm38/mm10 was used for comparison and annotation and fragments per kilobase million (FPKM) values were used as the standardized value output matrix for post data analysis.

The FPKM values of *Fxr*, *Shp*, and *Nr4a1* were selected to form a matrix based on the transcriptomics FPKM data matrix. Correlation analysis of data in R language by ggplot2 and ggpbur packages, where x-axis is set to *Shp* expression levels (FPKM) and y-axis is set to *Fxr* expression levels (FPKM) and *Nr4a1* expression levels (FPKM) respectively. Finally, the correlation between *Fxr*, *Nr4a1* and *Shp* is determined based on the R value, where the closer the absolute value of R is to 1, the stronger the linear correlation between the two variables.

Expression levels of genes involved in bile acids regulation. Mouse liver RNA extraction is the same as in transcriptomics. Reverse transcription kits were purchased from Bio-Rad Laboratories and reverse transcription was performed in a multifunctional PCR instrument according to the instructions. The reverse transcription conditions were: preheating at 25˚C for 10 min, reverse transcription at 37˚C for 2 h, reverse transcriptase inactivation at 85˚C for 5 min, and storage at 4˚C. Real Time Quantitative PCR (RT-qPCR) was performed by using 2*SYBR Green Supermix (Bio-Rad Laboratories, Inc.) on a CFX96 RT-PCR System (C1000 Touch; Bio-Rad Laboratories, Inc.). The RT-PCR parameters were as follows: 3 min, 95˚C and 1 cycle; 10 sec at 95˚C plus 45 sec at 60˚C, 40 cycles. The melting curve analysis consisted of 5 sec at 55˚C followed by heating up to 95˚C with a ramp rate of 0.5˚C/5 sec. Names and corresponding primer sequences of genes checked in the present study are in Table II. Expression levels of GAPDH in each sample were used as internal reference.

Liver (0.2 g) was ground into fine powder in liquid nitrogen, 1.1% formaldehyde solution was cross-linked for 15 min and 1.25 M glycine for 5 min terminated the cross-linking in the ice, the supernatant was centrifuged and resuspended twice in pre-cooled PBS. Then, 2 ml of frozen chromatin immunoprecipitation (ChIP) cell lysis buffer (containing 20 μl Protease inhibitors and 20 μl PMSF) was resuspended, ground 20 times on ice in a glass homogenizer, incubated on ice for 15 min and the supernatant was discarded by centrifugation at 4˚C, 1,000 x g, 5 min. Then, 1 ml of ChIP nuclear lysis buffer (containing 10 μl Protease inhibitors and 10 μl PMSF) was resuspended and incubated on ice for 5 min. Protease inhibitors and 10 μl PMSF) and incubate for 5 min on ice. The samples were sonicated on moist ice at 20% power for 2 sec with a 4 sec gap for a total of 6 min. The supernatant was divided into 120 μl tubes after centrifugation at 4˚C, 1,000 x g, 5 min and stored at -80˚C.

50 μl of ultrasound chromatin was added to 450 μl of ChIP dilution buffer (containing 2.25 μl Protease Inhibitor Cocktail II), and 5 μl (1%) was taken as Input and stored at 4˚C. 1 μg/μl IgG antibody (Millipore, 12-371) and 20 μl of mixed Protein G Magnetic Beads (Millipore, 16-662) were added to the negative control group. Add 2 μg/μl FXR antibody (Santa Cruz Biotechnology, sc-25309x) and 20 μl of well-mixed Protein G Magnetic Beads to the experimental group. The magnetic beads were separated from the liquid using a magnetic holder, and the supernatant was carefully pipetted into Low salt buffer, High salt buffer, and LiCl Wash buffer, respectively. For each sample (including Input samples), add 100 μl of freshly prepared Elution Buffer and 1 μl of Rnase A (10 mg/ml Solarbio, Beijing) in 37˚C water bath for 30 min with a shaking frequency of 300 rpm. Add 1 μl of proteinase K and shake at 300 rpm for 2 h. Incubate at 95˚C for 10 min and cool to room temperature. Separate the magnetic beads from the supernatant using a magnetic holder and carefully pipette the supernatant to a new 1.5 ml centrifuge tube. Purify the eluted DNA using the MinElute PCR Purification Kit (Qiagen, Germany 28006). The purified DNA was examined by ultra-micro spectrophotometer with 2 μl samples for DNA concentration, and 10 μl samples were examined by 1.2% agarose gel electrophoresis for chromatin fragments. Fluorescent quantitative PCR was performed using 2*SYBR Green Supermix. Primers are shown in Table III. pre-denaturation at 95˚C for 3 min, denaturation at 95˚C for 10 sec, extension at 60˚C for 45 sec, 40 cycles, and lysis curves were plotted. The results were compared with Input and then statistical analysis was performed with the expression value of IgG as the reference value.

Statistical analysis. All data were shown as mean ± standard error of the mean. Principal component analysis (PCA) was performed using the 'pca' function in the mixOmics package of the R program (http://mixomics.org/). Statistical significance levels tested by two-way ANOVA followed by a Tukey's test, which were performed by using the base functions 'aov' and 'TukeyHSD' in R program. The statistical significance levels of data were tested by the Student's t test, which was performed by using the base function 't.test' in R program. $P<0.05$ was considered to indicate a statistically significant difference. The raw sequence reads generated in the article have been

Table III. Primers used for chromatin immunoprecipitation-reverse transcription-quantitative PCR.

Gene	Forward primer (5' to 3')	Reverse primer (5' to 3')
Abcb11	TGCGTGGGGACCTTCTGAG	AGAGTCGGGCCTCTCACCA

uploaded to the NCBI BioProject database (https://www.ncbi.nlm.nih.gov/sra/) under accession number PRJNA885754.

Results

Biochemical index testing and HE staining. Metabolic disorders caused by HFD are accompanied by hyperglycemia, hypercholesterolemia and hyperlipidemia. Hypercholesterolemia is mainly manifested by abnormally high serum levels of TC and LDL-C. These two indicators were tested and it was shown that HFD significantly increased the expression levels of TC and LDL-C and the administration of GP treatment downregulated the expression of TC and LDL-C (Fig. 1A). HE staining showed that the HFD caused vacuolar-like lesions and irregular arrangement of hepatocytes. By contrast, the administration of GP and simvastatin (positive control drug) reduced the hepatocyte pathology-like lesions and neatly aligned cells (Fig. 1B), it was shown that the high-fat model was successfully constructed.

Metabolomics analysis of the effect of GP on the molecular level of bile acid. The bile acid profile in the liver, bile and serum of mice in the ND, HFD and GP groups was significantly different and the HFD-induced changes in the bile acids profile in the liver, bile and serum of mice. The bile acids profile of the liver, biliary and serum also changed following GP administration, ameliorating the changes caused by the HFD (Fig. 2) This suggested that GP has a therapeutic effect on changes in bile acids in mice caused by HFD.

In a further study, 16 bile acids were analyzed according to their bile acids structure into free bile acids, taurine-conjugated bile acids and glycine-conjugated bile acids. Based on our previous study (7), gypenosides decreased the CA/CDCA ratio which is positively related to cholesterol absorption and increasing CDCA levels suggested that gypenosides may accelerate hepatic free bile acid synthesis by promoting the key bile acid synthase. The changes in bile acids levels of 16 bile acids in bile and serum were further investigated (Fig. 3) and in serum, GP significantly altered the levels of DCA and LCA-free bile acids (Fig. 3A and D). LCA and DCA expression in the intestine is a key function of the intestinal microbiota (29), indicating that GP promotes the entry of bile acids into the blood and their absorption and expression in the intestine. Analysis of the levels of taurine-conjugated bile acids in bile and serum (Fig. 3B and E) showed that the results of changes in the levels of taurine-conjugated bile acids in the liver were similar to those in bile, with no significant differences in serum. The opposite expression was observed for the levels of glycine-conjugated bile acids in bile; presumably, GP promotes the transport of glycine-conjugated bile acids to the gallbladder. As glycine-conjugated bile acids were not detected in serum, only the effect of GP on the levels of

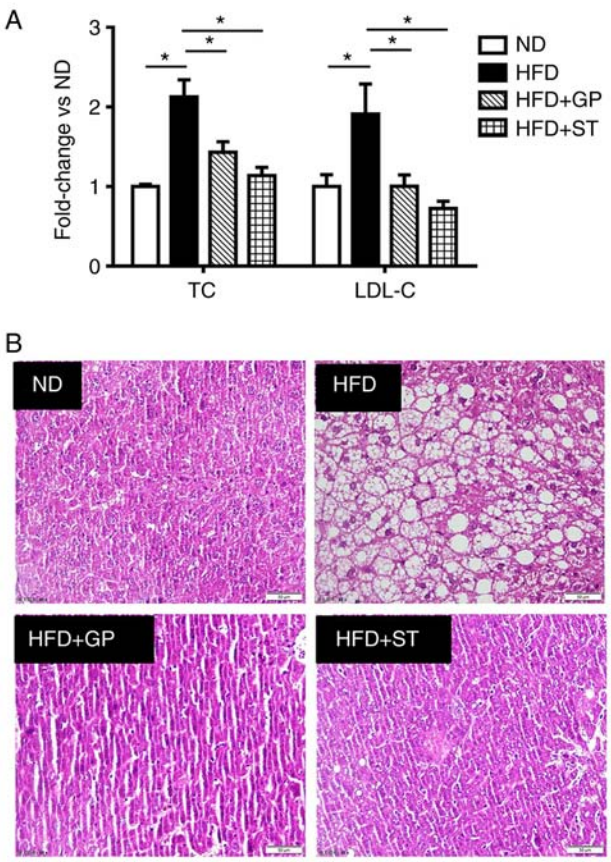

Figure 1. Effect of GP on lipid metabolism in mice. (A) GP regulates serum TC and LDL-C levels. (B) Histopathological examination of the liver (hematoxylin and eosin; magnification, x400). Data represent means ± standard error of the mean. n=5, *P<0.05. GP, gypenosides; TC, total cholesterol; LDL-C, low-density lipoprotein cholesterol; ND, normal diet; HFD, high fat diet; HFD + GP, GP treatment group; HFD + ST, simvastatin positive drug group.

glycine-conjugated bile acids in the liver and bile was analyzed in the present study (Fig. 3C). The increase in CDCA levels following the action of GP suggests that GP may increase the production of conjugated bile acids and facilitate the translocation of conjugated bile acids to the gallbladder by promoting the key bile acid synthase and the significant elevation of LCA and DCA in serum also demonstrates that GP also promote the entry of bile acids into the blood and their absorption and expression in the intestine.

Proteomics analysis of the effect of GP on the expression of bile acid pathway-related proteins. The effect of GP on the bile acids pathway in mouse liver was further explored by proteomics. In the present study, the bile acids-related proteins were queried by KEGG and NCBI databases and then a literature search conducted to screen 45 proteins closely related to

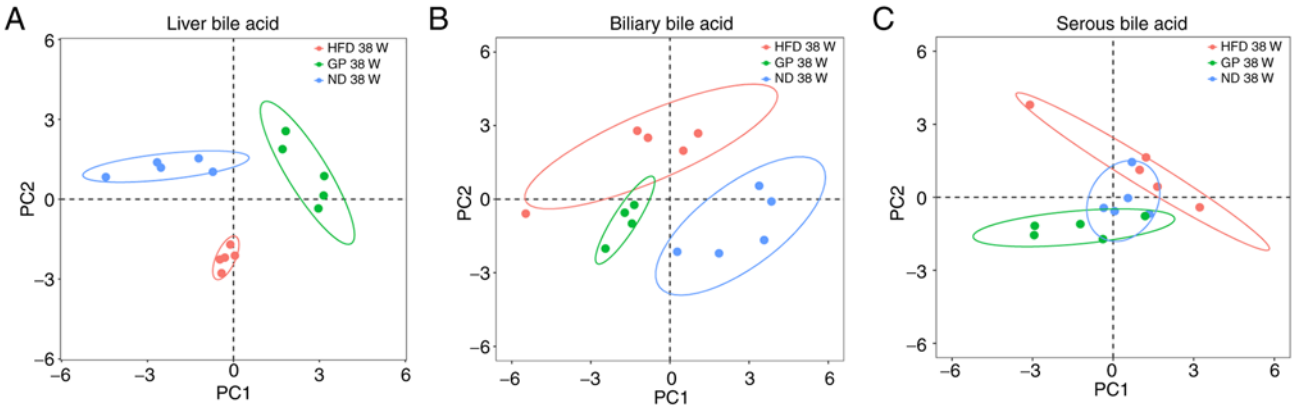

Figure 2. Principal component analysis. (A) Principal component analysis of liver bile acid. (B) Principal component analysis of biliary bile acid. (C) Principal component analysis of serous bile acid. n=5. Red represents 38 weeks of HFD; green represents 38 weeks of GP; blue represents 38 weeks of ND. HFD, high fat diet; GP, gypenosides/GP treatment; ND, normal diet.

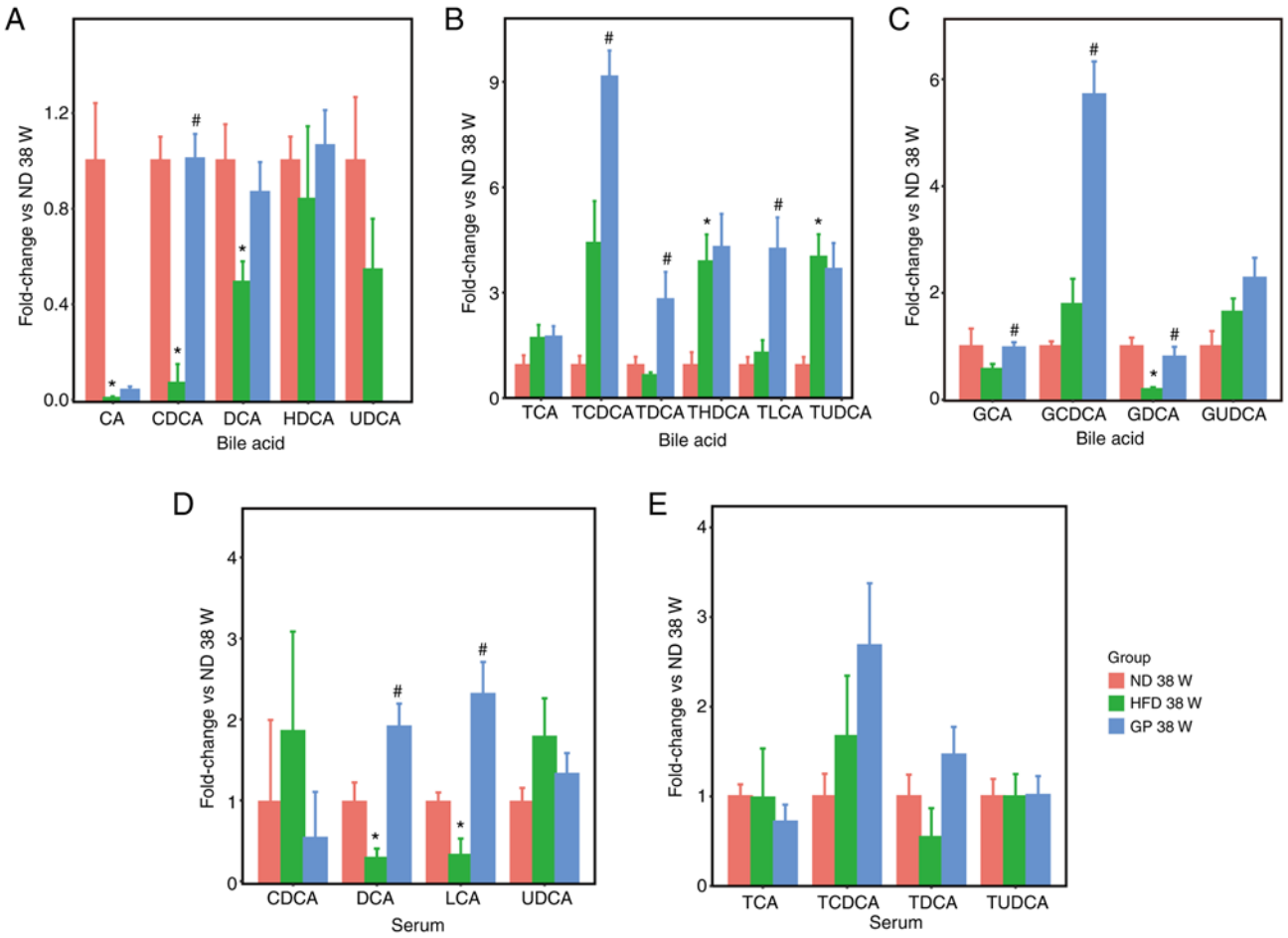

Figure 3. The effects of GP on the levels of bile acids with different structures in bile and serum. (A-C) The expression levels of free bile acids, taurine-conjugated bile acids, and glycine-conjugated bile acids in bile in bile acid, respectively. (D, E) The expression levels of free bile acids and taurine-conjugated bile acids in serum, respectively. Data represent means ± standard error of the mean. n=5, *P<0.05 HFD 38 W vs. ND 38 W, $^{\#}$P<0.05 GP 38 W vs. HFD 38 W. GP, gypenosides/GP treatment; HFD, high fat diet; W, weeks.

the bile acids synthesis, metabolism and transport pathways for analysis. The present study obtained 31 bile acids pathway proteins by high-resolution mass spectrometry and analyzed the expression of mouse liver bile acids pathway-related proteins after the effects of HFD and GP using volcano plots (Fig. 4). HSD17B4, AKR1D1 and AMACR were upregulated in response to HFD stress. CYP3A11, ABCB11, ABCC3, CYP8B1, ABCC2 and SLCO1A4 were significantly downregulated (Fig. 4A). It was hypothesized that HFD may cause hypercholesterolemia in mice through processes such as inhibition of bile acids synthesis and bile acids transport to the gallbladder. Following treatment with GP, mouse bile

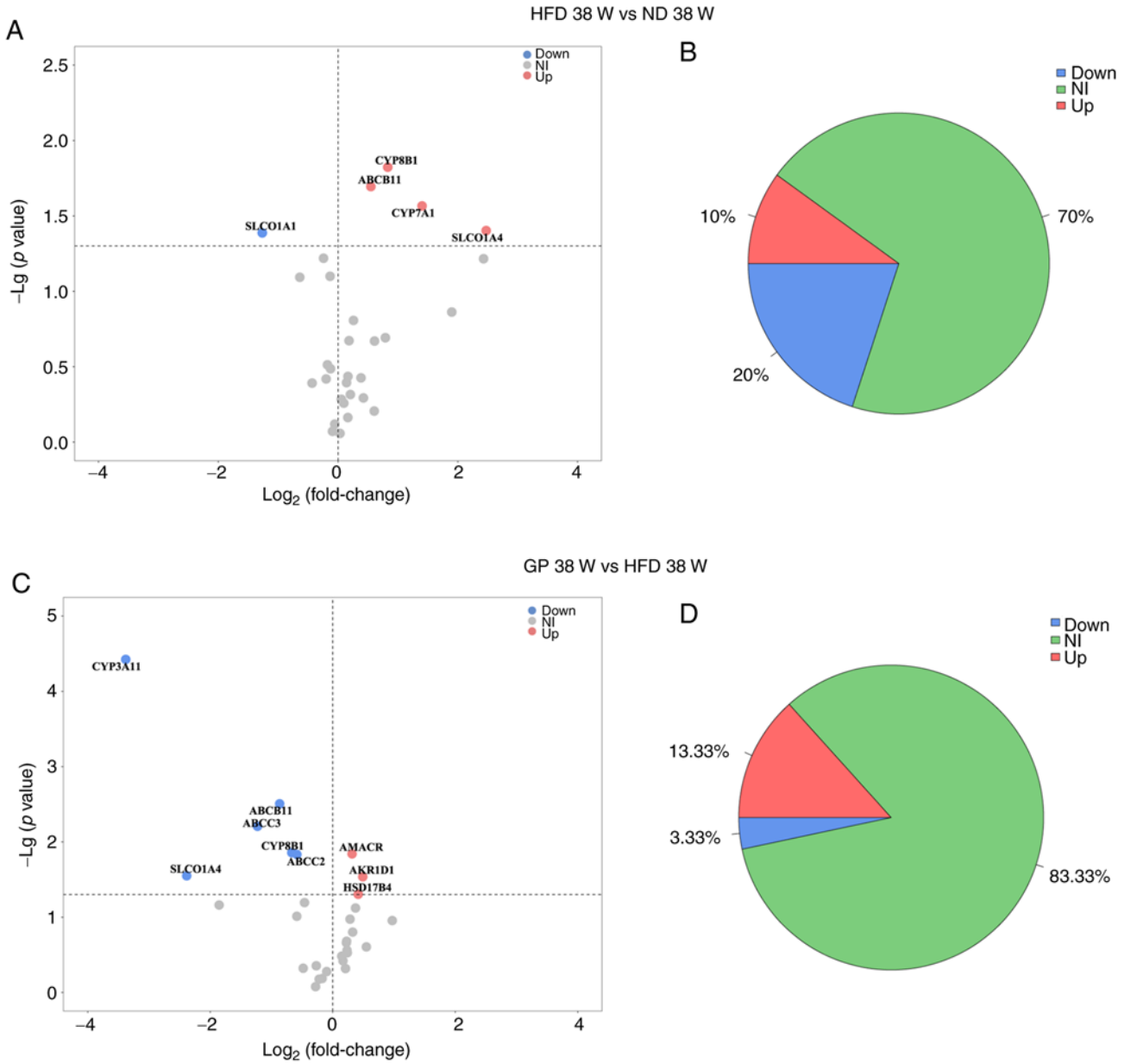

Figure 4. The effect of GP on expressions of bile acid pathway proteins in mice. Volcano plots showing the significantly regulated proteins. (A) In HFD vs. ND with volcano plot of differential proteins. (B) HFD vs. ND with pie chart. (C) In GP vs. ND with volcano plot of differentially expressed proteins. (D) GP diet vs. HFD with pie chart. The horizontal dashed line represents P<0.05. GP, gypenosides/GP treatment; HFD, high fat diet; ND, normal diet; W, weeks; NI, No impact.

acids pathway-related proteins CYP8B1, ABCB11, CYP7A1 and SLCO1A4 were significantly upregulated and SLCO1A1 was significantly downregulated (Fig. 4C). SLCO1A1 is responsible for the translocation and reabsorption of free bile acids from the blood into the liver (30,31), suggesting that GP may regulate hypercholesterolemia by promoting bile acids synthesis, further translocation of bile acids to the gallbladder and inhibition of bile acids reabsorption into the liver. Under HFD stress, significantly upregulated proteins accounted for 10% of the total bile acids pathway proteins and significantly downregulated proteins accounted for 20% of the total bile acids pathway proteins; following administration of GP (Fig. 4B), significantly upregulated proteins accounted for 13% of the total bile acids pathway proteins and significantly downregulated proteins accounted for 3% of the total bile acids pathway proteins (Fig. 4D). Thus it was shown that GP had a significant effect on bile acids pathway proteins in mice with the hypercholesterolemia model.

The present study performed association analysis for proteins that underwent significant changes (Fig. 5A). The horizontal coordinate represents the change in protein expression after the effect of a HFD and the vertical coordinate represents the change in protein expression after the effect of GP. The results showed that GP significantly downregulated the expression of SLCO1A4, CYP3A11, CYP8B1 and ABCB11 induced by HFD. HFD had significant effects on ABCC3, ABCC2, HSD17B4, AMACR, AKR1D1, CYP7A1 and SLCO1A1, which were also significantly regulated by GP. Selected proteins where GP significantly modulated the changes induced by a HFD were analyzed (Fig. 5C-H) and the results showed that the expression

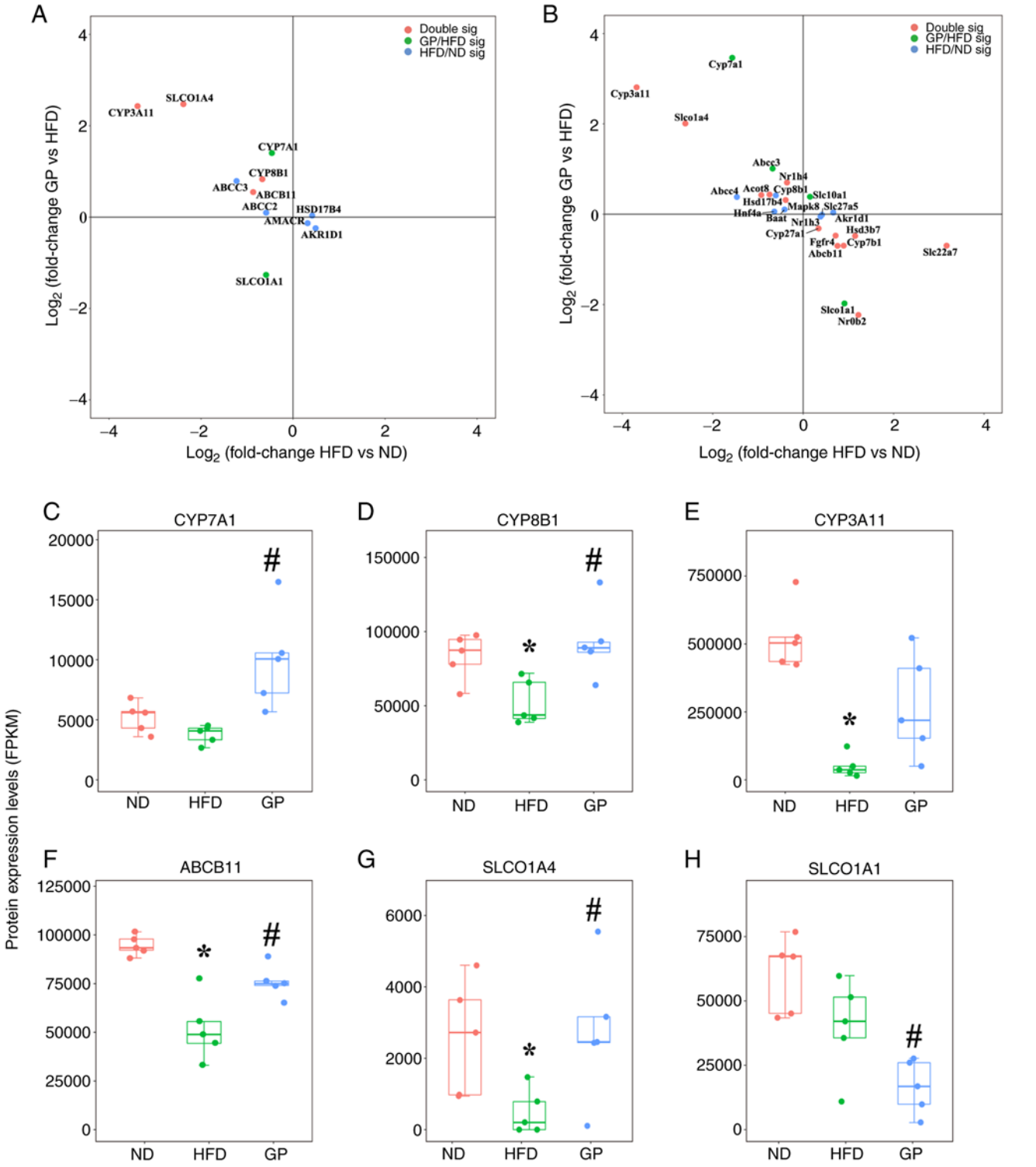

Figure 5. Differential analysis of bile acid proteins and genes by GP and the back-regulation of key proteins of the pathway. (A) Differential analysis of proteins in bile acid pathway on GP. (B) Differential analysis of genes in bile acid pathway on GP. (C-H) Regulation of CYP7A1, CYP8B1, CYP3A11, ABCB11, SLCO1A4, and CLCO1A1 key pathway proteins by GP. Data represent means ± standard error of the mean. n=5, *P<0.05 HFD 38 W vs. ND 38 W, $^{\#}$P<0.05 GP 38 W vs. HFD 38 W. Red represents 38 W of ND; Green represents 38 W of HFD; Blue represents 38 W of GP. GP, gypenosides/GP treatment; HFD, high fat diet; ND, normal diet; W, weeks; FPKM, fragments per kilobase million.

levels of CYP8B1, CYP3A11, ABCB11 and SLCO1A4 were significantly downregulated by HFD and the expression levels of CYP7A1, CYP8B1, ABCB11, SLCO1A4 were significantly upregulated, while the expression level of SLCO1A1 was significantly decreased. This is further evidence that GP promoted the expression level of CYP7A1, CYP8B1 and ABCB11 and increased bile acids synthesis and secretion to the bile duct. It was observed that GP inhibited the expression of SLCO1A1 and promoted the expression of CLCO1A4, indicating that GP increased the level of free bile acids in the blood and accelerated the excretion of free bile acids in the blood to the kidneys, thereby maintaining bile acids homeostasis.

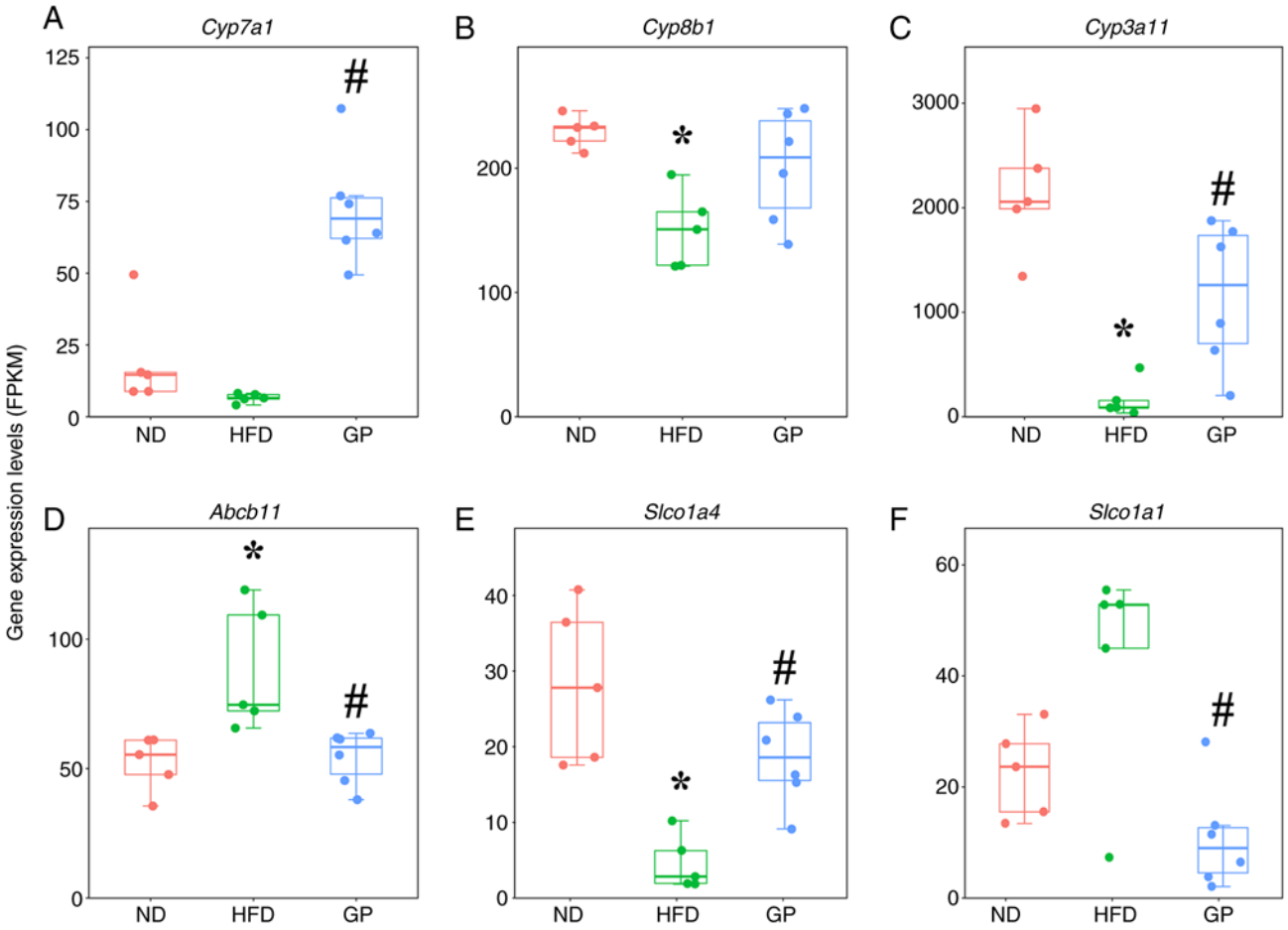

Figure 6. Differential analysis of gene in bile acids pathway on gypenosides. (A-F) Regulation of *Cyp7a1*, *Cyp8b1*, *Cyp3a11*, *Abcb11*, *Slco1a4*, and *Slco1a1* key pathway genes by gypenosides. Data represent means ± standard error of the mean. n=5, *P<0.05 HFD 38 W vs. ND 38 W, #P<0.05 GP 38 W vs. HFD 38 W. Red represents 38 W of ND; green represents 38 W of HFD; blue represents 38 W of GP. GP, gypenosides/GP treatment; HFD, high fat diet; ND, normal diet; W, weeks; FPKM, fragments per kilobase million.

Transcriptomics analysis of the effect of GP on the expression of bile acids-related genes. Proteomic analysis found that GP ameliorated the abnormal changes in proteins responsible for bile acids synthesis, metabolism and transport in the liver of mice affected by a HFD. The effect of GP on the expression of 45 bile acid pathway-related genes in mouse liver was further verified. These genes come from KEGG and NCBI databases. A total of 26 differentially expressed genes were screened using the volcano plots (Fig. S1) and association analysis was performed for these genes (Fig. 5B), with the horizontal coordinates representing gene expression changes after the effect of HFD and the vertical coordinates representing gene expression changes following GP, with the horizontal coordinates representing the changes in gene expression following the effects of HFD and the vertical coordinates representing the changes in gene expression following the effects of GP. Under HFD stress, GP caused significant upregulation of mRNA for *Cyp3a11, Slco1a4, Nr1h4, Acot8, Hsd17b4* and *Mapk8* and caused significant downregulation of mRNA for *Cyp27a1, Fgfr4, Abcb11, Cyp7a1, Hsd3b7, Slc22a7* and *Nr0b2*. In genes encoding bile acids pathway-related proteins, GP significantly reversed the mRNA expression of *Cyp7a1, Cyp3a11, Slco1a4, Abcb11* and *Slco1a1* (Fig. 6A-H) and tended to upregulate *Cyp8b1*, which was similar to the proteomic result. Further PCR validation of key genes on *Fxr* pathway showed that the expression of *Cyp7a1, Cyp8b1, Fxr, Aacb11* was significantly downregulated following GP treatment compared with HFD, but the expression of *Shp* was significantly decreased following GP treatment, which may be related to the treatment cycle of *Shp* (Fig. 7).

Effects of GP administration time on key genes and proteins of the FXR pathway. In addition to cholesterol metabolism via the bile acids pathway, cholesterol is also required for synthesis in the body, including steroid hormones, cell membranes and vitamin D. Therefore, to ensure that cholesterol is available for the rest of the physiological functions, the body may initiate feedback inhibition of *Cyp7a1* expression by the hepatic *Fxr* pathway, thus maintaining bile acids homeostasis. By studying the regulatory effects of GP on key genes and proteins such as *Fxr*, *Shp*, *Cyp7a1* and *Nr4a1* the effect of GP on the feedback regulation of bile acids in the liver *Fxr* pathway can be revealed (Fig. 8). Compared with the HFD group, the mRNA expression of *Cyp7a1* was significantly upregulated at 38 weeks and the expression level of this encoded protein was significantly upregulated at 18 and 38 weeks; the mRNA expression of *Fxr* was significantly downregulated at 18 weeks and significantly upregulated after 38 weeks and the expression level of its

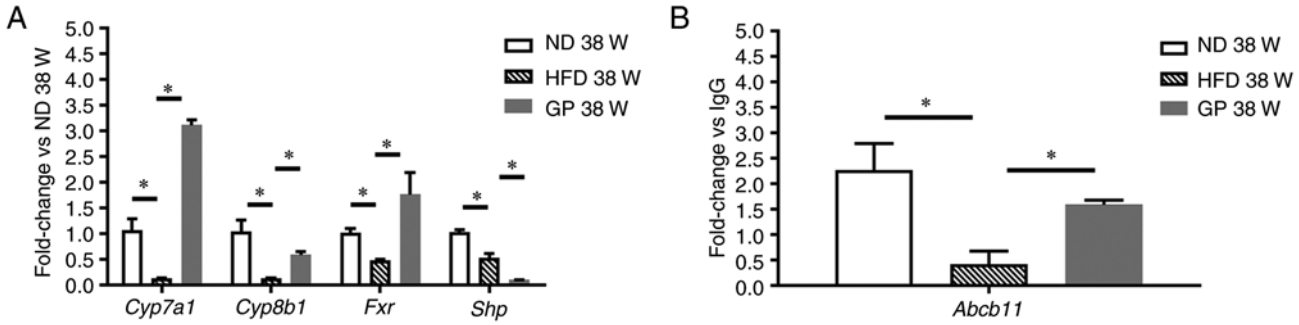

Figure 7. Expression of genes involved in the *Fxr* pathway. (A) *Cyp7a1*, *Cyp8b1*, *Fxr*, and *Shp* were detected by RT-qPCR, and (B) *Abcb11* gene was detected by CHiP-qPCR. Data represent means ± standard error of the mean. n=3, *P<0.05; RT-qPCR, reverse transcription-quantitative PCR; ChIP, chromatin immunoprecipitation; ND, normal diet; HFD, high fat diet; GP, GP treatment.

encoded protein was significantly upregulated at 32 weeks. However, at 26 and 32 weeks, it was significantly downregulated, probably due to organismal self-regulation; the mRNA expression of *Shp* was significantly downregulated after 38 weeks and the mRNA expression of *Nr4a1* was significantly downregulated at both 26 and 38 weeks. Since the protein expression of *Shp* and *Nr4a1* was not examined (possibly due to the low concentration of this protein in the group), only the transcript levels of *Shp* and *Nr4a1* were analyzed in the present study. Further correlation analysis of genes *Fxr*, *Nr4a1* and *Shp* (Fig. 8G and H) showed a significant negative correlation between *Fxr* and *Shp* (R=-0.633), while *Nr4a1* showed a significant positive correlation with *Shp* (R=0.800). GP may regulate cholesterol metabolism through *Nr4a1*-mediated FXR pathway.

Discussion

GP has the effect of regulating blood lipid and blood sugar levels and protecting the liver, which is of great clinical value in the treatment of obesity, fatty liver and metabolic diseases (32). The present study, using a hypercholesterolemic model mouse as the research object and using metabolomics, proteomics, transcriptomics and other multi-omics research tools, found that GP may accelerate the synthesis of bile acids by promoting the expression of key bile acids synthesis enzymes and increasing the expression of bile acids metabolizing enzymes to reduce the damage of bile acids to the liver. GP may also promote the expression of bile acids efflux transporters to accelerate the efflux of bile acids from the liver and inhibit the expression of bile acids uptake transporter to reduce bile acids reabsorption to the liver, which in turn promotes the excretion of bile acids into the kidney for detoxification and promotes the conversion of cholesterol to bile acids to maintain the homeostasis of the cholesterol-bile acids internal environment (Fig. 9). Unfortunately, the experiments were not performed for groups treated with GP on ND, but it will be included in future studies.

A combination of time course line (Fig. 8A-F) and PCR data used to analyze high-fat diet in the early stages: Low *Fxr* expression, low *Shp* expression and normal bile acid synthesis by *Cyp7a1*. In the late hyperlipidemic phase, bile acid accumulation activates *Fxr*, which increases *Shp* expression and thus inhibits *Cyp7a1*, limiting cholesterol catabolism and thus causing hypercholesterolemia. Significant increase in *Fxr* gene expression followed GP administration (Fig. 7). The significant decrease in *Shp* expression may be due to the fact that GP treatment is a slow process and the gene expression level of *Shp* had not recovered at the time point the material was collected (Fig. 9).

In the liver, CYP7A1 and CYP8B1 protein expression levels, as well as mRNA expression of the genes encoding these proteins, were downregulated under HFD stress, consistent with literature reports (33-35), suggesting that a HFD inhibits liver metabolism and causes the development of hypercholesterolemia (36).The upregulation of the expression levels of CYP7A1 and CYP8B1 and the mRNA expression of the genes encoding these proteins following the action of GP may cause an increase in the concentration of 7α-hydroxycholesterol, a catalytic reaction product of 7α-hydroxylase and induce the processing modification of enzymes such as CYP8B1, thereby promoting liver cholesterol metabolism and producing primary bile acids. It was also observed by UPLC-MS analysis that the levels of free bile acids such as CDCA, UDCA and DCA in mouse liver increased following the administration of GP, indicating that one of the mechanisms by which GP lowers hepatic cholesterol may be through promoting the expression of CYP7A1 and CYP8B1, the key bile acid synthesis enzymes, to accelerate the synthesis of free bile acids and thus promote the metabolism of hepatic cholesterol. *Nr1h3* expression was significantly increased under HFD (Fig. 5B) and HFD can cause metabolic disorders with hypercholesterolemia. Unfortunately, a limitation of the present study was that it did search for alterations in SREBP levels.

The bile acids efflux transporter protein ABCB11 is the main transporter protein for hepatic secretion of bile salts and ABCB11 is the rate-limiting enzyme of the entire enterohepatic cycle (37), which efficiently transports bound bile acids across the hepatocyte parietal membrane and pumps them through the bile ducts into the gallbladder by stimulating the formation of bile salt-dependent bile flow (17). HFD decreases ABCB11 expression (38) and in humans ABCB11 mutations lead to severe intrahepatic cholestasis. ABCB11 protein expression is significantly reduced in patients with nonalcoholic steatohepatitis (39), consistent with *Abcb11* mRNA experimental results in the present study (Fig. 7B). In the present study, GP could alleviate HFD-induced liver injury by promoting the expression of ABCB11 and accelerating the secretion of

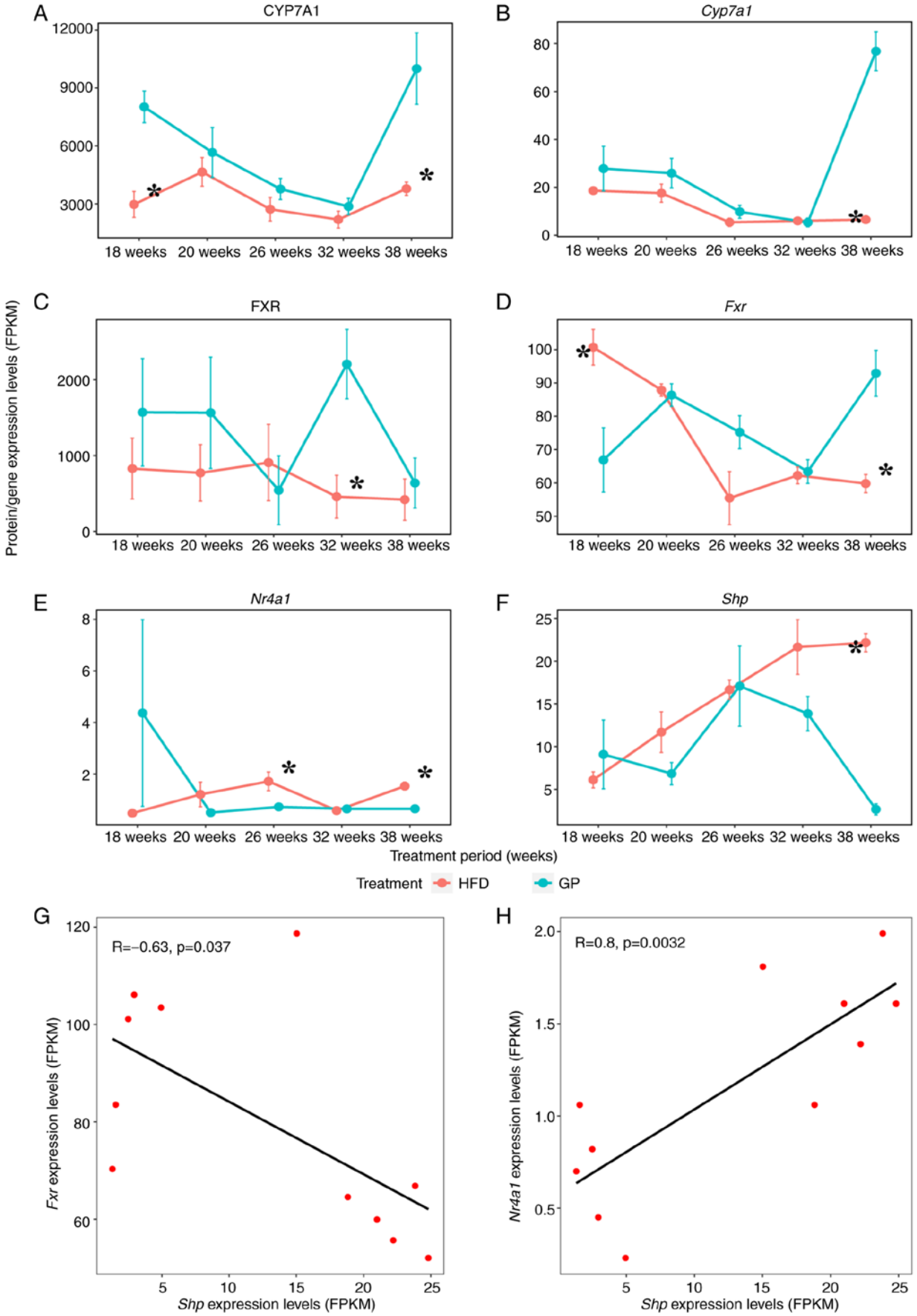

Figure 8. Effects of administration time on FXR pathway and correlation comparison. (A-F) Time course of key gene and protein expression levels in the FXR pathway at each identical time point GP vs. HFD for CYP7A1, *Cyp7a1*, FXR, *Fxr*, *Nr4a1*, *Shp*. Data represent means ± standard error of the mean. n=5, *P<0.05 HFD 18 W vs. GP 18 W, *P<0.05 HFD 20 W vs. GP 20 W, *P<0.05 HFD 26 W vs. GP 26 W, *P<0.05 HFD 32 W vs. GP 32 W, *P<0.05 HFD 38 W vs. GP 38 W. (G, H) Correlation analysis of mRNA expression of *Fxr*, *Nr4a1*, and *Shp*. FXR, farnesoid X receptor; HFD, high fat diet; GP, GP treatment; HFD, high fat diet; CYP7A1, cholesterol 7α-hydroxylase; FPKM, fragments per kilobase million.

hepatic conjugated bile acids into the bile ducts. Meanwhile, the analysis of UPLC-MS results showed that the levels of GCDCA and GDCA in liver were significantly decreased following the administration of GP, while the levels of GCA, GCDCA and GDCA in bile were significantly increased, indicating that GP could alleviate the liver injury caused by HFD by promoting the expression level of ABCB11 protein and accelerating the secretion of liver-bound bile acids into the bile ducts. In addition, the present study found that ABCB11 was inconsistently expressed at the transcriptional and protein levels, possibly due to GP indirectly regulating the expression of ABCB11.

Bile acids transporters SLCO1A1 and SLCO1A4 are members of the OATP family. SLCO1A1 is responsible for transporting free bile acids from the blood for reabsorption back to hepatocytes and SLCO1A4 transports free bile acids from hepatocytes into the blood (40). In the present study, the expression of SLCO1A1 protein as well as its encoding gene was significantly reduced in the hypercholesterolemic model mice following GP intervention, while the expression of SLCO1A4 protein as well as its encoding gene was significantly increased, suggesting a reduction in free bile acids reabsorption into the liver and facilitation of free bile acids transport to the body circulation in the liver. In the present study, bile acids reabsorption was inhibited, therefore, it was hypothesized that the bile acids entering the kidney through blood circulation was increased, thus preventing bile acids reabsorption into the liver and causing bile stasis and reducing the toxic effect on liver cells. It is worth mentioning that previous studies found that increased fecal bile acids were accompanied by increased hepatic bile acids synthesis (41,42). By inhibiting SLCO1A1 and promoting SLCO1A4 expression, GP reduced the reabsorption of hepatic free bile acids and accelerated the entry of hepatic free bile acids into the bloodstream for excretion into the kidney through blood circulation, which may be another mechanism to promote bile acids metabolism and lower hepatic cholesterol.

CYP3A11, homologous to human CYP3A4 and a bile acids metabolic enzyme, is mainly responsible for converting hydrophobic bile acids such as LCA, DCA and CDCA into hydrophilic bile acids by hydroxylation (43), enhancing their water solubility for excretion and thus maintaining the internal environment homeostasis of bile acids. The results of the present study showed that a HFD induced a decrease in CYP3A11 protein expression levels and mRNA expression levels of its encoding gene. Following the administration of GP, CYP3A11 protein expression levels and mRNA expression levels of its encoding gene were increased, resulting in increased water solubility of bile acids and accelerated excretion of bile acids. Thus, GP avoids biliary stasis and liver injury by promoting hepatic bile acids hydroxylation, which in turn promotes bile acids metabolism and excretion.

GP promotes CYP7A1-catalyzed hepatic cholesterol metabolism for the synthesis of bile acids, and hepatic cholesterol levels decrease (44). In addition to cholesterol metabolism through the bile acids pathway, besides being metabolized by the bile acid pathway, cholesterol is also required for the synthesis of steroid hormones, cell membranes, and vitamin D in the body (45) and to ensure that cholesterol can meet the needs of the remaining physiological functions, the body

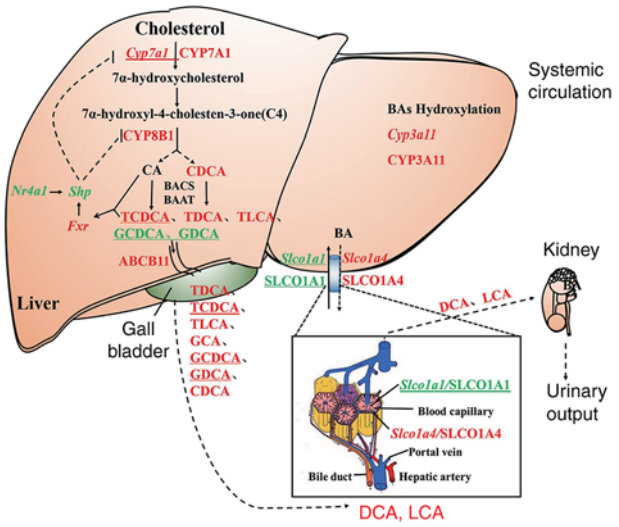

Figure 9. The regulation of GP on genes and proteins expression in bile acid pathway in mice liver. Capital letters represent proteins, lowercase italics represent genes; red represents the expression is significantly downregulated by high-fat diet and upregulated by GP; green represents the expression is significantly upregulated by high-fat diet and downregulated by GP; the underline represents no significant change in high-fat diet and GP significantly modulates; black represents no change in either. GP, gypenosides/GP treatment; CYP7A1, Cholesterol 7α-hydroxylase; CYP8B1, Oxysterol-7α-hydroxylase; CA, cholic acid; BACS, bile acid-CoA synthase; BAAT, amino acid N-acyltransferase; TCDCA, taurochenodeoxycholic acid; TDCA, tauroursodeoxycholic acid; TLCA, taurolithocholic acid; GCDCA, glycochenodeoxycholic acid; GDCA, glycodeoxycholic acid; ABCB11, bile salt export pump; GCA, glycocholic acid; CDCA, chenodeoxycholic acid; SLCO1A1, solute carrier organic anion transporter family member 1A1; SLCO1A4, solute carrier organic anion transporter family, member 1A4; DCA, deoxycholic acid; LCA, lithocholic acid.

may initiate feedback inhibition of the hepatic FXR pathway for CYP7A1 expression, thus maintaining the homeostasis of the cholesterol-bile acids internal environment. Under normal physiological conditions, bile acids are the catalytic products of CYP7A1 and have a negative feedback regulation on their expression (46,47). Endogenous bile acid CDCA is the most potent ligand of FXR (48,49), which increases the expression of SHP by activating FXR and inhibiting bile acids synthesis (50,51).

Activation of FXR increases the expression of SHP and NR4A1, another nuclear receptor in the body, which can indirectly regulate glycolipid metabolism by regulating the transcription factor SHP (52). In the present study, the correlation analysis of *Fxr* and *Nr4a1* with *Shp* using transcriptomic data revealed that the regulatory effect of *Nr4a1* on *Shp* was stronger than that of *Fxr* on *Shp*. GP may further inhibit the expression of *Shp* by suppressing the expression of *Nr4a1*, while upregulating the expression levels of *Cyp7a1*, as well as its encoded protein, to promote hepatic cholesterol metabolism. Synthesis of CDCA and TCDCA levels increased, which in turn promoted *Fxr* expression. GP may improve bile acids metabolism and maintain the dynamic cholesterol-bile acids balance by regulating the *Nr4a1*-mediated bile acids metabolic pathway. *Nr4a1* expression was reduced following GP treatment and *Shp* expression was reduced (Fig. 8E and F), which in turn further accelerated *Cyp7a1* catabolism of cholesterol and alleviated hypercholesterolemia. The bile acid pathway

mediated by *Nr4a1*, another nuclear receptor in the liver, may be another mechanism to maintain the homeostasis of bile acids.

Research has shown that glycine-conjugated bile acids are predominant in human serum. Taurine-conjugated bile acids predominate in the serum of odontocetes (53). Through extensive literature search none was found stating that glycine-conjugated bile acids are not present in the liver and bile. Glycine-conjugated bile acids are not detected in serum probably because they are hydrolyzed in the intestine by bile salt hydrolases (BSHs), which hydrolyze the amide bond and release the glycine/taurine molecule from the steroid via the intestinal microbiota (54). Studies have shown that BSHs preferentially hydrolyze glycine-conjugated bile acids (55,56), so glycine-conjugated bile acids are hydrolyzed in the intestine, leading to a decrease in their absorption into the blood, which may be one of the reasons why it was not possible to measure glycine-conjugated bile acids in the serum of mice. Conjugated bile acids of the glycine/taurine conjugated bile acids exhibit a different dynamic balance in the circulatory system (57).

In summary, GP mainly regulates the synthesis, metabolism and transport of bile acids and hepatic NR4A1-mediated bile acids pathway by regulating the expression of key bile acids synthases CYP7A1 and CYP8B1, bile acids metabolizing enzyme CYP3A11, major bile acids efflux and uptake transporters ABCB11, SLCO1A4 and SLCO1A1 at the transcriptional or protein level to maintain internal environment homeostasis for bile acids, which in turn regulates the bile acids pathway, promotes hepatic cholesterol metabolism and lowers hepatic cholesterol.

Acknowledgements

Not applicable.

Funding

The present study was supported by the National Nature Science Foundation of China (grant nos. 82260843 and 82060649), Guizhou Provincial Postgraduate Research Fund Project [grant no. QJH YJSKYJJ (2021)186], the Science and Technology Foundation of Guizhou Province of China [grant nos. QKHPTRC (2017)5733-060 and QKHPTRC (2017)5733-062] and the Doctoral Research Start-up Fund Project of Zunyi Medical University (grant no. F-938).

Availability of data and materials

The datasets used and/or analyzed during the current study are available from the corresponding author on reasonable request.

Authors' contributions

CCF wrote the manuscript and analyzed data. YPY and AJL established the mice model and collected tissue samples. LQ, DPT, YLL and YQH designed the present study, contributed to interpretation of the data and revised the manuscript. CCF and YPY confirm the authenticity of all the raw data. All authors read and approved the final manuscript.

Ethics approval and consent to participate

All procedures involving the use of laboratory animals were in accordance with the requirements of Animal Experiment Ethics Committee of Zunyi Medical University (approval no. 2-557).

Patient consent for publication

Not applicable.

Competing interests

The authors declare that they have no competing interests.

References

1. Yu JN, Cunningham SR, Thouin T, Gurvich D and Liu D: Hyperlipidemia. Prim Care 27: 541-587, 2000.
2. Bunnoy A, Saenphet K, Lumyong S, Saenphet S and Chomdej S: Monascus purpureus-fermented Thai glutinous rice reduces blood and hepatic cholesterol and hepatic steatosis concentrations in diet-induced hypercholesterolemic rats. BMC Complement Altern Med 15: 88, 2015.
3. Karr S: Epidemiology and management of hyperlipidemia. Am J Manag Care 23: 139-148, 2017.
4. Collins R, Reith C, Emberson J, Armitage J, Baigent C, Blackwell L, Blumenthal R, Danesh J, Smith GD, DeMets D, *et al*: Interpretation of the evidence for the efficacy and safety of statin therapy. Lancet 19: 2532-2561, 2016.
5. Sessa M, Rafaniello C, Scavone C, Mascolo A, di Mauro G, Fucile A, Rossi F, Sportiello L and Capuano A: Preventable statin adverse reactions and therapy discontinuation. What can we learn from the spontaneous reporting system? Expert Opin Drug Saf 17: 457-465, 2018.
6. Livingstone SJ, Looker HC, Akbar T, Betteridge DJ, Durrington PN, Hitman GA, Neil HA, Fuller JH and Colhoun HM: Effect of atorvastatin on glycaemia progression in patients with diabetes: An analysis from the collaborative atorvastatin in diabetes trial (CARDS). Diabetologia 59: 299-306, 2016.
7. Lu Y, Du Y, Qin L, Wu D, Wang W, Ling L, Ma F, Ling H, Yang L, Wang C, *et al*: Gypenosides altered hepatic bile acids homeostasis in mice treated with high fat diet. Evid Based Complement Alternat Med 2018: 8098059, 2018.
8. Megalli S, Aktan F, Davies NM and Roufogalis BD: Phytopreventative anti-hyperlipidemic effects of gynostemma pentaphyllum in rats. J Pharm Pharm Sci 8: 507-515, 2005.
9. Attawish A, Chivapat S, Phadungpat S, Bansiddhi J, Techadamrongsin Y, Mitrijit O, Chaorai B and Chavalittumrong P: Chronic toxicity of Gynostemma pentaphyllum. Fitoterapia 75: 539-551, 2004.
10. Chiranthanut N, Teekachunhatean S, Panthong A, Khonsung P, Kanjanapothi D and Lertprasertsuk N: Toxicity evaluation of standardized extract of Gynostemma pentaphyllum Makino. J Ethnopharmacol 149: 228-234, 2013.
11. Lazarević S, Đanić M, Goločorbin-Kon S, Al-Salami H and Mikov M: Semisynthetic bile acids: A new therapeutic option for metabolic syndrome. Pharmacol Res 146: 104333, 2019.
12. Staley C, Weingarden AR, Khoruts A and Sadowsky MJ: Interaction of gut microbiota with bile acid metabolism and its influence on disease states. Appl Microbiol Biotechnol 101: 47-64, 2017.
13. Vallim TQdA, Tarling EJ and Edwards PA: Pleiotropic roles of bile acids in metabolism. Cell Metab 17: 657-669, 2013.
14. Malhi H and Camilleri M: Modulating bile acid pathways and TGR5 receptors for treating liver and GI diseases. Curr Opin Pharmacol 37: 80-86, 2017.
15. Trauner M, Fuchs D, Halilbasic E and Paumgartner G: New therapeutic concepts in bile acid transport and signaling for management of cholestasis. Hepatology 65: 1393-1404, 2017.
16. Zhang L, Wang Q, Liu W, Liu F, Ji A and Li Y: The orphan nuclear receptor 4A1: A potential new therapeutic target for metabolic diseases. J Diabetes Res 2018: 9363461, 2018.
17. Dawson PA and Oelkers P: Bile acid transporters. Curr Opin Lipidol 6: 109-114, 1995.

18. Meier PJ, Eckhardt U, Schroeder A, Hagenbuch B and Stieger B: Substrate specificity of sinusoidal bile acid and organic anion uptake systems in rat and human liver. Hepatology 26: 1667-1677, 1997.
19. Modica S, Gadaleta RM and Moschetta A: Deciphering the nuclear bile acid receptor FXR paradigm. Nucl Recept Signal 8: e005, 2010.
20. Goodwin B, Jones SA, Price RR, Watson MA, McKee DD, Moore LB, Galardi C, Wilson JG, Lewis MC, Roth ME, *et al*: A regulatory cascade of the nuclear receptors FXR, SHP-1, and LRH-1 represses bile acid biosynthesis. Mol Cell 6: 517-526, 2000.
21. Chiang JY, Kimmel R, Weinberger C and Stroup D: Farnesoid X receptor responds to bile acids and represses cholesterol 7alpha-hydroxylase gene (CYP7A1) transcription. J Biol Chem 275: 10918-10924, 2000.
22. Hu YW, Zhang P, Yang JY, Huang JL, Ma X, Li SF, Zhao JY, Hu YR, Wang YC, Gao JJ, *et al*: Nur77 decreases atherosclerosis progression in apoE(-/-) mice fed a high-fat/high-cholesterol diet. PLoS One 9: e87313, 2014.
23. Jung YS, Lee HS, Cho HR, Kim KJ, Kim JH, Safe S and Lee SO: Dual targeting of Nur77 and AMPKα by isoalantolactone inhibits adipogenesis in vitro and decreases body fat mass in vivo. Int J Obes (Lond) 43: 952-962, 2019.
24. Kudo T, Nakayama E, Suzuki S, Akiyama M and Shibata S: Cholesterol diet enhances daily rhythm of Pai-1 mRNA in the mouse liver. Am J Physiol Endocrinol Metab 287: E644-E651, 2004.
25. Abdou HS, Robert NM and Tremblay JJ: Calcium-dependent Nr4a1 expression in mouse Leydig cells requires distinct AP1/CRE and MEF2 elements. J Mol Endocrinol 56: 151-161, 2016.
26. De Fabiani E, Mitro N, Anzulovich AC, Pinelli A, Galli G and Crestani M: The negative effects of bile acids and tumor necrosis factor-alpha on the transcription of cholesterol 7alpha-hydroxylase gene (CYP7A1) converge to hepatic nuclear factor-4: A novel mechanism of feedback regulation of bile acid synthesis mediated by nuclear receptors. J Biol Chem 276: 30708-30716, 2001.
27. He Y, Yang T, Du Y, Qin L, Ma F, Wu Z, Ling H, Yang L, Wang Z, Zhou Q, *et al*: High fat diet significantly changed the global gene expression profile involved in hepatic drug metabolism and pharmacokinetic system in mice. Nutr Metab (Lond) 17: 37, 2020.
28. Zhang Y and Klaassen CD: Effects of feeding bile acids and a bile acid sequestrant on hepatic bile acid composition in mice. J Lipid Res 51: 3230-3242, 2010.
29. Kakiyama G, Pandak WM, Gillevet PM, Hylemon PB, Heuman DM, Daita K, Takei H, Muto A, Nittono H, Ridlon JM, *et al*: Modulation of the fecal bile acid profile by gut microbiota in cirrhosis. J Hepatol 58: 949-955, 2013.
30. Wood M, Ananthanarayanan M, Jones B, Wooton-Kee R, Hoffman T, Suchy FJ and Vore M: Hormonal regulation of hepatic organic anion transporting polypeptides. Mol Pharmacol 68: 218-225, 2005.
31. Miyazaki H, Sekine T and Endou H: The multispecific organic anion transporter family: Properties and pharmacological significance. Trends Pharmacol Sci 25: 654-662, 2004.
32. Zhang H, Chen X, Zong B, Yuan H, Wang Z, Wei Y, Wang X, Liu G, Zhang J, Li S, *et al*: Gypenosides improve diabetic cardiomyopathy by inhibiting ROS-mediated NLRP3 inflammasome activation. J Cell Mol Med 22: 4437-4448, 2018.
33. He X, Zheng N, He J, Liu C, Feng J, Jia W and Li H: Gut microbiota modulation attenuated the hypolipidemic effect of simvastatin in High-Fat/cholesterol-diet fed mice. J Proteome Res 16: 1900-1910, 2017.
34. Yu L, Lu H, Yang X, Li R, Shi J, Yu Y, Ma C, Sun F, Zhang S and Zhang F: Diosgenin alleviates hypercholesterolemia via SRB1/CES-1/CYP7A1/FXR pathway in high-fat diet-fed rats. Toxicol App Pharmacol 412: 115388, 2021.
35. Gillard J, Clerbaux LA, Nachit M, Sempoux C, Staels B, Bindels LB, Tailleux A and Leclercq IA: Bile acids contribute to the development of non-alcoholic steatohepatitis in mice. JHEP Rep 4: 100387, 2022.
36. Gryn SE and Hegele RA: Ezetimibe plus simvastatin for the treatment of hypercholesterolemia. Expert Opin Pharmacother 16: 1255-1262, 2015.
37. Ren T, Pang L, Dai W, Wu S and Kong J: Regulatory mechanisms of the bile salt export pump (BSEP/ABCB11) and its role in related diseases. Clin Res Hepatol Gastroenterol 45: 101641, 2021.
38. Okushin K, Tsutsumi T, Ikeuchi K, Kado A, Enooku K, Fujinaga H, Yamauchi N, Ushiku T, Moriya K, Yotsuyanagi H and Koike K: Heterozygous knockout of Bile salt export pump ameliorates liver steatosis in mice fed a high-fat diet. PLoS One 15: e0234750, 2020.
39. Okushin K, Tsutsumi T, Enooku K, Fujinaga H, Kado A, Shibahara J, Fukayama M, Moriya K, Yotsuyanagi H and Koike K: The intrahepatic expression levels of bile acid transporters are inversely correlated with the histological progression of nonalcoholic fatty liver disease. J Gastroenterol 51: 808-818, 2016.
40. Kalliokoski A and Niemi M: Impact of OATP transporters on pharmacokinetics. Br J Pharmacol 158: 693-705, 2009.
41. Herrema H, Meissner M, Dijk TH, Brufa G, Boverhof R, Oosterveer MH, Reijngoud DJ, Müller M, Stellaard F, Groen AK and Kuipers F: Bile salt sequestration induces hepatic de novo lipogenesis through farnesoid X receptor- and liver X receptor alpha-controlled metabolic pathways in mice. Hepatology 51: 806-816, 2010.
42. Out C, Hageman J, Bloks VW, Gerrits H, Gelpke MDS, Bos T, Smit MJ, Kuipers F and Groen AK: Liver receptor homolog-1 is critical for adequate up-regulation of Cyp7a1 gene transcription and bile salt synthesis during bile salt sequestration. Hepatology 53: 2075-2085, 2011.
43. Chen J, Zhao KN and Chen C: The role of CYP3A4 in the biotransformation of bile acids and therapeutic implication for cholestasis. Ann Transl Med 2: 7, 2014.
44. Cao K, Zhang K, Ma M, Ma J, Tian J and Jin Y: Lactobacillus mediates the expression of NPC1L1, CYP7A1, and ABCG5 genes to regulate cholesterol. Food Sci Nutr 9: 6882-6891, 2021.
45. Maekawa M: Domain 4 (D4) of perfringolysin O to visualize cholesterol in cellular membranes-the update. Sensors (Basel) 17: 504-518, 2017.
46. Lorbek G, Lewinska M and Rozman D: Cytochrome P450s in the synthesis of cholesterol and bile acids-from mouse models to human diseases. FEBS J 279: 1516-1533, 2012.
47. Chiang JYL: Bile acids: Regulation of synthesis. J Lipid Res 50: 1955-1966, 2009.
48. Makishima M, Okamoto AY, Repa JJ, Tu H, Learned RM, Luk A, Hull MV, Lustig KD, Mangelsdorf DJ and Shan B: Identification of a nuclear receptor for bile acids. Science 284: 1362-1365, 1999.
49. Li G and Guo GL: Farnesoid X receptor, the bile acid sensing nuclear receptor, in liver regeneration. Acta Pharm Sin B 5: 93-98, 2015.
50. Xiang D, Yang J, Liu Y, He W, Zhang S, Li X, Zhang C and Liu D: Calculus bovis sativus improves bile acid homeostasis via Farnesoid X receptor-mediated signaling in rats with estrogen-induced cholestasis. Front Pharmacol 10: 48, 2019.
51. Zhang Y, Jackson JP, St Claire RL III, Freeman K, Brouwer KR and Edwards JE: Obeticholic acid, a selective farnesoid X receptor agonist, regulates bile acid homeostasis in sandwich-cultured human hepatocytes. Pharmacol Res Perspect 5: 329-340, 2017.
52. Miao L, Yang Y, Liu Y, Lai L, Wang L, Zhan Y, Yin R, Yu M, Li C, Yang X and Ge C: Glycerol kinase interacts with nuclear receptor NR4A1 and regulates glucose metabolism in the liver. FASEB J 33: 6736-6747, 2019.
53. Wahlström A, Sayin SI, Marschall HU and Bäckhed F: Intestinal crosstalk between bile acids and microbiota and its impact on host metabolism. Cell Metab 24: 41-50, 2016.
54. Begley M, Hill C and Gahan CG: Bile salt hydrolase activity in probiotics. App Environs Microbiol 72: 1729-1738, 2006.
55. Tanaka H, Hashiba H, Kok J and Mierau I: Bile salt hydrolase of Bifidobacterium longum-biochemical and genetic characterization. App Environ Microbiol 66: 2502-2512, 2000.
56. Kim GB, Miyamoto CM, Meighen EA and Lee BH: Cloning and characterization of the bile salt hydrolase genes (bsh) from Bifidobacterium bifidum strains. App Environ Microbiol 70: 5603-5612, 2004.
57. Yang T, Shu T, Liu G, Mei H, Zhu X, Huang X, Zhang L and Jiang Z: Quantitative profiling of 19 bile acids in rat plasma, liver, bile and different intestinal section contents to investigate bile acid homeostasis and the application of temporal variation of endogenous bile acids. J Steroid Biochem Mol Biol 172: 69-78, 2017.